THE ASTROPHYSICAL JOURNAL, 411:869–873, 1993 July 10

BROAD-BAND X-RAY TELESCOPE OBSERVATIONS OF THE MAGNETIC CATACLYSMIC VARIABLE H0538+608 = BY CAMELOPARDALIS

T. R. KALLMAN. E. M. SCHLEGEL, P. J. SERLEMITSOS, R. PETRE, F. MARSHALL, K. JAHODA, E. A. BOLDT, S. S. HOLT, R. F. MUSHOTZKY, J. SWANK, A. E. SZYMKOWIAK, R. L. KELLEY, A. SMALE, K. ARNAUD, AND K. WEAVER
Laboratory for High Energy Astrophysics, NASA/Goddard Space Flight Center, Greenbelt, MD 20771
AND
F. B. PAERELS
Department of Physics, University of California, Berkeley, CA 94720
Received 1992 October 5; accepted 1993 January 20

ABSTRACT

We report on BBXRT observations of the cataclysmic variable H0538+608 (=BY Cam). The unexcelled energy resolution of BBXRT in the vicinity of the iron K line allows the line strength and energy to be constrained more tightly than has previously been possible. We are able to rule out a significant contribution from fluorescence on iron more neutral than Fe XVIII. Implications for the conditions in the accreting gas are discussed.

Subject headings: novae, cataclysmic variables — stars: individual (BY Camelopardalis) — X-rays: stars

1. INTRODUCTION

The system H0538+608 (=BY Cam) is a notable AM Her–type (or "polar") cataclysmic variable. Objects of this class consist of a magnetized white dwarf in orbit with a late-type companion. The class is defined by the high degree of circular and linear polarization and the synchronization of the white dwarf spin period with the orbital period. These objects are typically characterized by a large soft X-ray to hard X-ray flux ratio, and by a much higher X-ray-to-optical ratio than other CV classes. This suggests that the dominant energy release occurs in the X-ray band pass, while other wavelengths are affected by reprocessed radiation. X-rays are thus of particular importance to AM Her stars, and many of the 18 currently known polars were discovered by X-ray satellites.

Polars as a class serve as an accretion laboratory. Most of the accretion energy is expected to be liberated in the polar region, since the accreting material is constrained to these regions by the strong magnetic field. A shock forms in the accretion region, above the surface of the white dwarf star. Early models were pictured as an accretion column, but more recent models involve an accretion curtain or an arc (Cropper 1990). The accretion energy is expected to be divided among three main components: (1) optical cyclotron emission emitted from the accretion column directly; (2) soft X-ray emission ($kT \sim 40$ eV) from the white dwarf surface; and (3) optically thin, hard X-ray emission from the postshock region. We still do not understand how the accretion energy is divided among these components. The soft X-ray component is believed to be reprocessed hard X-rays, yet an "excess" is present, based upon models matching the observed luminosities of the other two components, for many systems. This excess has become known as the soft X-ray problem.

H0538+608 was discovered by the *HEAO 1* A2 experiment and has been variously named 4U 0541+60 (Forman et al. 1978) and 1H 0533+607 (Wood et al. 1984). Identification as an AM Her object, by Remillard et al. (1986), was based on color and variability, and confirmed by polarimetry. From the polarization variations, Mason, Liebert, & Schmidt (1989) obtained a relatively precise period of 3.331 ± 0.015 hr. The ultraviolet spectrum shows unusual line ratios characteristic of old novae (Bonnet-Bidaud & Mouchet 1987). Observations with *EXOSAT* revealed a chaotically varying light curve (Shrader et al. 1988), soft X-ray eclipses, and no evidence for the "soft excess" problem which occurs in other AM Her objects. However, these observations did not have sufficient spectral resolution to rule out a soft component with flux equal to or greater than that of the hard X-rays. This ambiguity was due in part to the uncertainty in the interstellar absorption toward H0538+608. H0538+608 is the third-brightest-known AM Her star in the hard (≥1 keV) X-ray band. *Ginga* observations revealed the existence of two luminosity states: a "flaring" state with an average luminosity of 1.4×10^{32} ergs s^{-1}, and a "pulsing" state with a luminosity of 9.2×10^{31} ergs s^{-1} (for the 1.8–37 keV band, with an assumed distance of 100 pc). There is also a strong iron K emission line near 6.4–6.8 keV (Ishida et al. 1989).

This paper presents the BBXRT spectrum of H0538+608. The energy resolution allows us to separate the iron K complex into components emitted at different sites, and to measure or set limits on the strengths of these lines. The result will lead to new constraints on possible emission models.

2. RESULTS

2.1. *The BBXRT Observation*

The Broad-Band X-Ray Telescope (BBXRT) experiment consists of two coaligned conical mirrors with solid-state detectors at each focus (Serlemitsos et al. 1991). It was flown as part of the *Astro 1* payload on the space shuttle during 1990 December 2–11. The instrument covers the 0.3–12 keV band, at a resolution of $\Delta E = 150$ eV. The central pixel is 4′ in diameter.

H0538+608 was observed for about 2500 s on day 5 of the mission, 1990 December 7. H0538 was centered in the field of view of both telescopes to within 1.′17. The optics spread ~20% of the photons into the outer pixels of the detectors. The observation was contiguous and was almost entirely

during orbital night. The average counting rate was 1.3 s^{-1} in the "A" detector, and 0.84 s^{-1} in the "B" detector. An examination of the *EXOSAT* field for H0538+608 revealed no additional source, or any extended component, with the BBXRT field of view.

2.2. *Continuum Fitting*

We have fitted the data from H0538+608 with a model spectrum consisting of thermal bremsstrahlung emission together with an iron line and low-energy photoelectric absorption. The data were binned so that there were at least 15 counts per bin. This binning, for the most part, affected the extrema in energy, namely, the lowest and highest energy bins. Since BBXRT is not sensitive to photon energies greater than 10 keV, we fixed the bremsstrahlung temperature at the value found by the *Ginga* satellite $kT = 30$ keV (Ishida et al. 1989). With this choice, we find χ^2/degree of freedom = 227.6/238 for our best fit. We find a less good fit ($\chi^2 = 245.1/238$) to a single, absorbed power-law spectrum with an index of 0.38 in energy. The total flux is $3.9 \pm 7 \times 10^{-11}$ ergs cm^{-2} s^{-1} in the 2–10 keV energy band. In the 1.8–37.4 keV (*Ginga*) band, the flux is 4.8×10^{-11} ergs cm^{-2} s^{-1}, corresponding to a luminosity of 5.4×10^{31} ergs s^{-1} at a distance of 100 pc. The best-fit bremsstrahlung spectrum is shown in Figure 1.

2.3. *Absorption*

The column density of neutral material required in order to fit to the BBXRT data is $1.0^{+3.0}_{-1.0} \times 10^{20}$ cm^{-2}. In addition, the data require the presence of an absorption edge at $0.55^{+0.06}_{-0.12}$ keV with an optical depth of $0.5^{+0.6}_{-0.3}$. We can also test whether the data are consistent with the presence of a soft blackbody component. We find that the upper limit on the flux of such a component is 5.4×10^{-12} ergs cm^{-2} s^{-1} in the 0.18–0.8 keV band, for a blackbody temperature $kT_{BB} = 50$ eV. This may be compared with the flux from the hard X-rays in the 2–10 keV band that we infer, which is 3.69×10^{-11} ergs cm^{-2} s^{-1}. Owing to its lack of sensitivity below about 0.5 keV, BBXRT is of limited value in constraining a blackbody component with temperature much lower than this value.

H0538+608 was also detected by the low-energy detectors on the *EXOSAT* satellite (Shrader et al. 1988). For this data the sensitivity to much lower energy X-rays (~0.1 keV) results in more severe constraints on the luminosity of a possible soft component, although the poorer energy resolution results in weaker constraints on the absorbing column. Figure 2 shows the χ^2 contours for various values of 50 eV blackbody flux (relative to the hard X-ray component) and column density derived from simultaneous fits to the *EXOSAT* medium-energy and low-energy detector data taken during 1985. We show the constraints on L(BB)/L(brems) implied by two separate ME spectra taken 12 hr apart, and the simultaneous fluxes measured with the low-energy experiment, using the thin Lexan and Aluminum-Parylene filters, as a function of the assumed column density. These results are consistent with the BBXRT fits and show that the blackbody luminosity must be less than 10% of the hard X-ray luminosity if the column derived from BBXRT is correct. If the added absorption above the oxygen K edge is due to partial ionization of the absorbing gas, then it is possible that the true opacity below 0.5 keV would be smaller than the standard interstellar value (Morrison & McCammon 1983) used in these fits. Under these conditions it is likely that the true blackbody luminosity is still smaller than that implied by Figure 2.

These fits can also be compared with the predictions of the interstellar column based on the reddening toward H0538+608. Bonnet-Bidaud & Mouchet (1987) estimate $E_{B-V} \leq 0.05$ from the absence of a 2200 Å feature in the ultraviolet spectrum taken with *IUE*; this corresponds approximately to an interstellar neutral hydrogen column density of $\leq 2.9 \times 10^{20}$ cm^{-2} (Savage & Mathis 1979). This is comparable to the column derived from the BBXRT fits.

2.4. *Iron Line Fitting*

The unexcelled energy resolution of BBXRT in the 6–8 keV region allows us to constrain both the energy and the width of the iron line much more tightly than has been possible before. We find a best-fit line energy of $6.6^{+0.09}_{-0.07}$ keV, an equivalent width of 500 ± 148 keV, and a line width $\sigma = 0.23^{+0.07}_{-0.08}$ keV. Figure 3 shows the contours of constant χ^2 for the centroid energy and width of the iron line. This shows that we can rule out a narrow ($\sigma \leq 0.05$ keV) line at the 90% confidence level. We can also rule out the presence of 6.4 and 6.9 keV lines, as χ^2

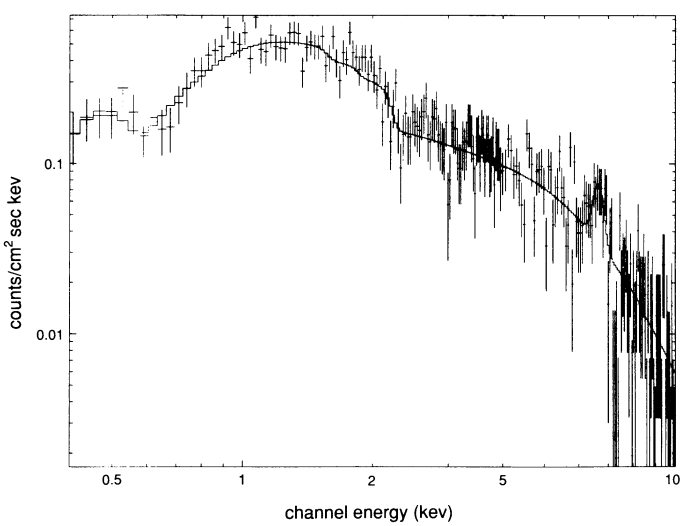

FIG. 1.—BBXRT spectrum of H0538+608 = BY Cam (*crosses*), together with the best-fit spectrum described in the text (*solid curve*).

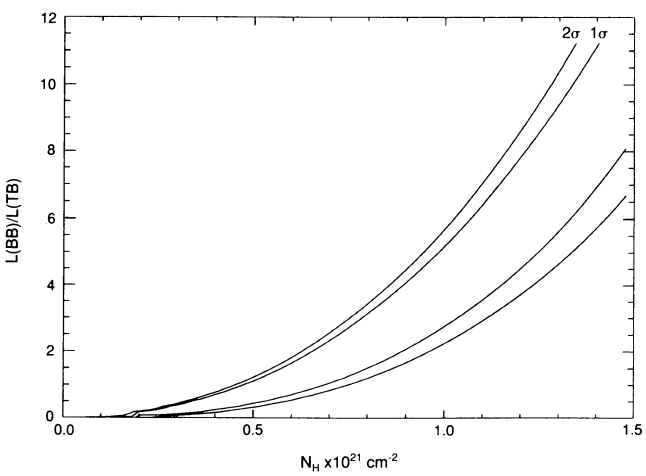

FIG. 2.—The χ^2 contours for the normalization of a 50 eV blackbody and the absorbing column for the 1985 *EXOSAT* data. The blackbody normalization has been converted to the ratio of soft to hard X-ray luminosity. The constraints are given for data taken on 1985, day 281 (ME + LE/thin Lexan filter). The 1 σ and 2 σ contours are labeled on one side of the most probable region.

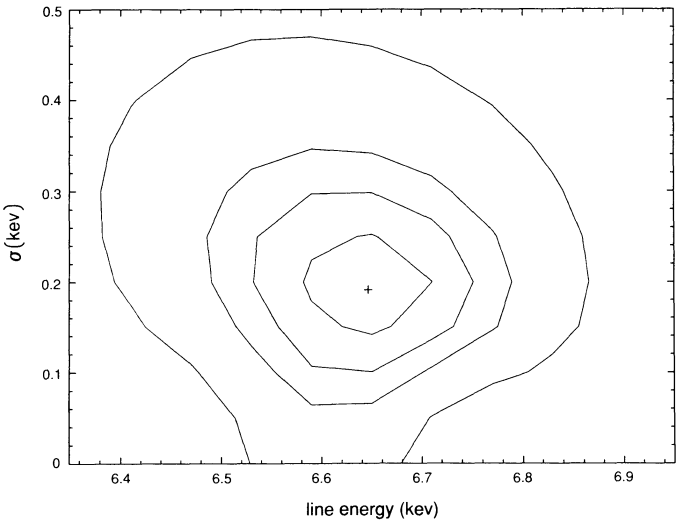

FIG. 3.—The χ^2 contours for the iron line width and line center from the best-fit spectrum. Contours correspond to 1 σ intervals about the χ^2 minimum.

increases by about 10 from the fitted minimum. If we test the data against a model consisting of a (narrow) 6.6 keV line together with either a (narrow) 6.4 or 6.9 keV component, we can set an upper limit of 10% on the strength of a 6.4 keV component and 30% on the strength of a 6.9 keV component, relative to the 6.6 keV component. Figure 4 shows the spectrum in the vicinity of the iron line, together with fits for one line component.

2.5. *Timing and Variability*

No variability is apparently present in the BBXRT observation. A power spectrum analysis found no power at any reasonable frequency throughout the observation. The orbital phase at which the BBXRT observation was made is difficult to determine. The phasing of H0538+608 has still not been established with a high degree of confidence. *If* the best ephemeris (Mason et al. 1989) can be used, then the BBXRT observation occurred from ~0.4 to ~0.6 in orbital phase. However, a recent study by Silber et al. (1992) shows that the orbital period (determined by a narrow Hα eclipse) differs by 3.05 minutes from the spin period of the white dwarf, which had previously been taken to be the orbital period. Given the number of cycles since the period was determined (~12,000), considerable error has built up.

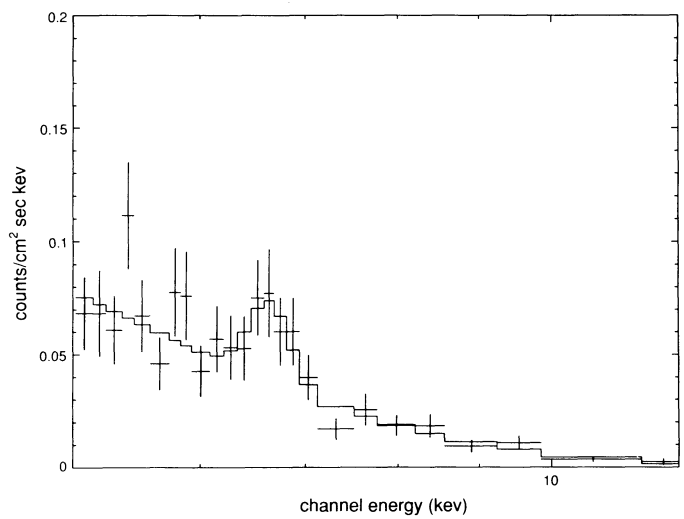

FIG. 4.—BBXRT spectrum of H0538+608 in the vicinity of the iron line

3. DISCUSSION

Although the detailed physical conditions in the accretion column depend on unknown quantities such as the magnetic field geometry and the gas dynamics in the flow, the radiation emitted by reprocessing at the white dwarf surface can be estimated relatively easily. The spectrum can be crudely represented by a blackbody with a temperature of $T_{WD} \sim (F/\sigma)^{1/4} \sim 5.1 \times 10^4 (F/4 \times 10^{-14}$ ergs s^{-1} cm$^{-2})^{1/4}$, where F is the incident flux from the shock or the column and σ is the Stefan-Boltzmann constant.

Of great interest is the expected emission at various temperatures from the iron lines in the 6.4–6.9 keV range. Ishida et al. (1989) found the iron line at 6.6 ± 0.1 keV with a line strength which varied with the spin phase, becoming strongest at spin phase ~0.75. As discussed in Ishida et al., four sites are possible: the postshock region, the preshock region, the white dwarf surface, and the companion. As Ishida et al. point out, the companion can be eliminated as a site, as the predicted behavior does not match the observations. The postshock region, with a temperature of ~30 keV, is expected to produce an iron line at ~6.9 keV with an equivalent width of ~120 eV. An iron line at 6.4 keV is expected from the white dwarf surface and the preshock region. A combination of the two lines was proposed first by Swank, Fabian, & Ross (1984). The BBXRT spectrum states that a combination of the 6.5 and 6.9 keV lines do not describe the observed line. The observed equivalent width is quite high relative to the predictions, suggesting that the observed line *is* a blend, but not a blend of 6.4 and 6.9 keV emission. As described in the previous section, the observed line could be a blend of the 6.6 and 6.9 keV lines, with the dominant emission coming from the former component. We also point out that the BBXRT spectrum had limited phase coverage, so our results may not be completely representative of the system.

We can estimate the conditions in the accretion flow implied by the line energy we measure. If the reprocessing material is assumed to be a cylinder with vertical thickness h and radius $R_c = R(f)^{1/2}$, where R is the white dwarf radius and f is the fraction of the surface covered by the emission region, then the ionization parameter in the reprocessor is $\xi = L/R^2 fn$ and the column density in the reprocessor is $N = nh$. If the mean density of the reprocessor is determined by free-fall accretion with a rate $\dot{M} = L/\eta c^2$, then the mean density is $n = 1.6 \times 10^9$ cm$^{-3} \eta^{-1} f^{-1} m^{-1/2} R_8^{-3/2} (L/5 \times 10^{32})$, the ionization parameter is $\xi = 6.3 \times 10^7$ ergs cm s$^{-1} n m^{1/2} R_8^{-1/2}$, and the column density is $N = 1.6 \times 10^{17}$ cm$^{-2} \eta^{-1} f^{-1}$ $(h/R) m^{-1/2} R_8^{-1/2} (L/5 \times 10^{32})$. In these equations η is the efficiency with which accreted material is converted into radiation, R_8 is the white dwarf radius in units of 10^8 cm, $L/5 \times 10^{32}$ is the luminosity in units of 5×10^{32} ergs s^{-1}, and m is the white dwarf mass in units of 1 $M_\odot$.

In Figure 5 we show the ion fractions expected for optically thin gas photoionized by a 30 keV bremsstrahlung spectrum. From this figure it is apparent that the ion stages implied by the fit to the observed line, Fe XXII–Fe XXV, occur at $\log(\xi) = 2.1$–2.5. The equivalent width we observed requires a reprocessor column density of $\geq 10^{23}$ cm^{-2} (cf. Makishima 1986; Kallman 1991). Both these constraints can be satisfied if $\eta \simeq 1.3 \times 10^{-5}$ and $f \simeq 6.3 \times 10^{-3} (h/R)$, or $\eta \simeq 8 \times 10^{-6}$ and

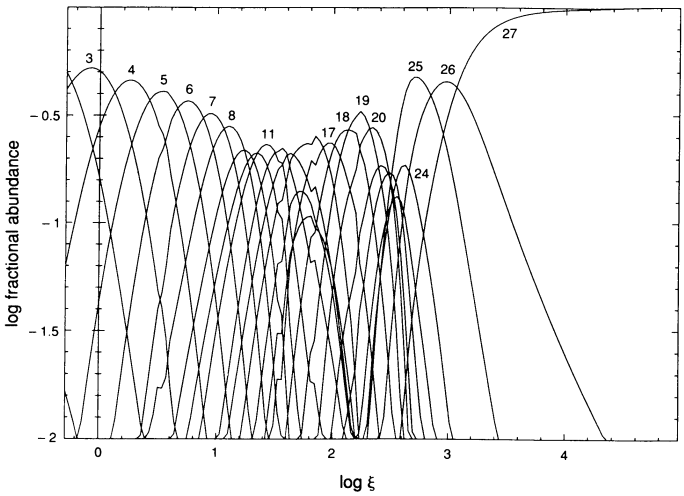

FIG. 5.—Iron ion abundances as a function of the ionization parameter of an optically thin gas for a 30 keV bremsstrahlung ionizing spectrum.

$f \simeq 8 \times 10^{-3}(h/R)$, for $m = 0.5$ and $R_8 = 9$ or $m = 1$ and $R_8 = 6$, respectively (using the mass-radius relationship for fully degenerate white dwarfs). We can demonstrate this in more detail by calculating a synthetic spectrum for such conditions, using the XSTAR photoionization code (Kallman & McCray 1982; Kallman & Krolik 1993). Figure 6 shows the results of a fit to the BBXRT spectrum of H0538+608 consisting of a 30 keV bremsstrahlung spectrum and reprocessed emission from a slab of gas with column density 4×10^{23} cm^{-2} and ionization parameter log (ξ) = 2.4. The fit to the iron line can only be achieved, however, if the line-emitting gas is more highly obscured than the bremsstrahlung continuum. This is because at ionization parameters such as these the gas also emits strong K lines and edges of Si, S, Ar, and Ca, and these are not present at their required strengths in the observed spectrum. Thus, the reprocessed emission shown in Figure 6 is subject to an added absorption by a column of 2.5×10^{22} cm^{-2}.

The values for accretion efficiency η that we derive from these models can be compared with the maximum theoretical

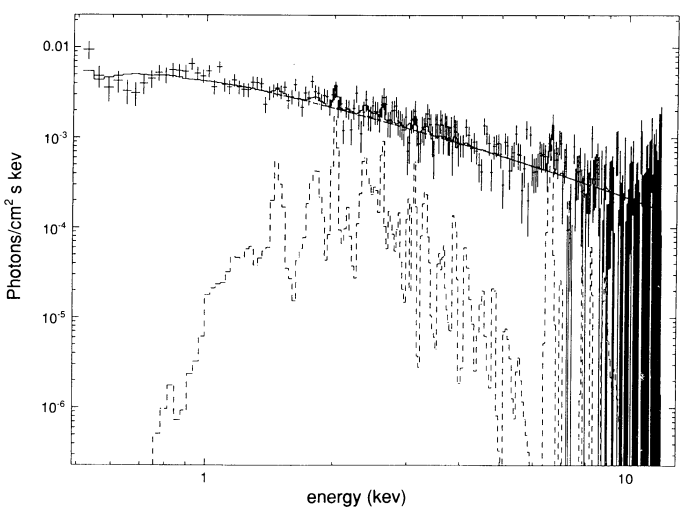

FIG. 6.—Fit to the BBXRT spectrum of H0538+608 (*crosses*) consisting of a 30 keV bremsstrahlung spectrum (*solid curve*) and reprocessed emission from a slab of gas with column density 4×10^{23} cm^{-2} and ionization parameter log (ξ) = 2.4 (*dashed curve*). The reprocessed emission is subject to an added absorption by a column of 2.5×10^{22} cm^{-2}.

efficiency, $\eta_{max} = 1.5 \times 10^{-3} m/R_8$, giving $\eta/\eta_{max} = 0.16$ and 0.03 for $m = 0.5$ and 1, respectively. Since these values are much less than unity, it is likely that a significant fraction of the accreting gas does not participate in hard X-ray production. An alternative mechanism for the loss of kinetic energy of most of the accreting material is by soft X-ray emission. This can occur, for example, if the accreting particles fall directly into the white dwarf crust without prior deceleration, and so give their energy locally to the thermal energy of the white dwarf atmosphere, resulting in strong soft X-ray emission. Such deceleration is also likely to result in little or no iron K-line production, since the infalling material will be slowed primarily by collisions. This can account for the absence of a 6.4 keV component to the iron line. However, such a scenario is still likely to result in soft X-ray emission and will thus violate the limits on a soft component we derived in § 2.3.

In principle, η/η_{max} rises with decreasing white dwarf mass, at a fixed value of the ionization parameter in the reprocessor, due to the strong dependence of η_{max} on $m(\eta/\eta_{max} = 2 \times 10^{-4}\xi_m^{-2}$, using the M-R relation for white dwarfs), and therefore assuming a low mass for the white dwarf might bring η/η_{max} up to unity. For the measured value $\xi \sim 200$, the white dwarf mass would have to be as low as $m \sim 0.2$ in order to achieve the maximum efficiency. However, such a low mass is clearly ruled out by *Ginga*'s measurement of the shock temperature, which requires the object to be more massive than $m \sim 0.7$ (Ishida et al. 1989).

The strong irradiation of the white dwarf photosphere by hard X-rays emitted by the shocked accretion stream will also result in fluorescent iron K emission from near-neutral material, at 6.4 keV. The equivalent width of the line has been calculated to be $\sim 420\ (\Omega/4\pi)$ eV for 20 keV bremsstrahlung irradiation spectrum (Hatchett & Weaver 1977; Basko 1977), where Ω is the solid angle subtended by the white dwarf as seen by the shock. The fluorescent photons are subject to Compton downscattering as they escape the atmosphere, leaving a fraction 0.75–0.40 (depending on chemical composition, with the higher number applying to cosmic abundances) unscattered photons in a narrow line. This reduces the equivalent width of the narrow line to $\leq 320\ \Omega/4\pi$ eV. This can be brought into accord with our results if $\Omega/4\pi \leq 0.3$, consistent with a shocked region of moderate extent above the white dwarf surface. Alternatively, the shock could be thin ($\Omega/4\pi = \frac{1}{2}$ as envisaged in standard models for the accretion region), but the fluorescent photons could arise in a hot, highly ionized layer on the white dwarf surface of optical depth ≥ 1 in the iron K continuum, so that they are emitted at energies above 6.4 keV.

The width of the iron line can also be used to constrain conditions in the accretion flow. The best fit to the observed spectrum requires a width of 0.23 keV and excludes a single narrow component. The most likely explanations for such a width include blending of multiple narrow lines from various ionization stages of iron, thermal Doppler broadening, Doppler broadening by bulk motions of the emitting gas, or Compton scattering. Blending cannot be ruled out in the absence of higher resolution spectra. Thermal Doppler broadening is expected to produce a width which is far too small to account for the observations, $\sigma_{Thermal} \simeq 1.7 \times 10^{-3} T_7^{1/2}$ keV, where T_7 is the gas temperature in units of 10^7 K. Bulk Doppler motions can account for the observed width if the velocity is $v \simeq 10^4$ km s^{-1}. Such velocities are somewhat greater than the largest physical velocity which is likely to occur in this system, the free-fall velocity onto the surface of the white dwarf. This is 6650 km s^{-1} for $m = 1$, and

3840 km s^{-1} for $m = 0.5$. Compton scattering is expected to produce a broadening of $\sigma \simeq \tau(0.187 + 0.0134T_7)$ keV, and a centroid shift of $\Delta\epsilon \simeq \tau(-0.24 + 0.0088T_7)$, where τ is the Thomson optical depth. This estimate is obtained by fitting the Monte Carlo calculations of Pozdnyakov, Sobol, & Sunyaev (1979); note that an earlier publication of this relation by one of us (Kallman & White 1989) contains an error in the coefficient of temperature. Note also that these formulae are somewhat misleading owing to the fact that when the Thomson depth exceeds unity, or when the temperature approaches 10^8 K, the scattered line profile is likely to differ significantly from the shifted and broadened Gaussian shape we used to fit the data. Nonetheless, the observed iron line width and centroid energy are crudely consistent with Compton scattering if the Thomson optical depth is approximately 1, and the temperature is $\simeq 2 \times 10^8$ K. These constraints cannot be satisfied in the line-emitting gas itself, since at such temperatures iron is likely to be nearly completely ionized and the line energy will be near 7 keV. However, it is possible that scattering in a medium which is separate from the main iron line emission site could provide the observed broadening. More accurate tests of this hypothesis, and of the effects of line blending on the profile shape, must await observations with greater spectral resolution.

The energy of the absorption edge near 0.6 keV is consistent with that expected from oxygen, ranging from neutral to 3 times ionized. This suggests that the absorption is occurring in a medium which is either partially ionized, or in which the abundance of oxygen is enhanced relative to other elements. The equivalent hydrogen column implied by this edge is 6.5×10^{20} cm^{-2} for solar abundances, so that an oxygen abundance enhancement of a factor ≈ 6 is required if the material is neutral. It is worthy of note that the UV spectrum shows anomalously weak emission in the C IV λ1550 line, relative to the N V λ1240 and Si IV λ1300 lines (Bonnet-Bidaud & Mouchet 1987), which could be indicative of the abundance anomalies required to account for the 0.6 keV absorption edge. If the absorber is "warm," that is, partially ionized (cf. Krolik & Kallman 1984), then it is difficult to account for the low energy of the edge; ionization sufficient to suppress the carbon and helium opacity relative to oxygen would likely raise the mean ionization state of oxygen beyond O^{+3}, and hence would not account for the edge energy we measure. Tests of model warm absorbers in comparison with the BBXRT spectra bear this out. However, the details of such models depend sensitively on the shape of the ionizing spectrum, particularly at energies below the BBXRT band pass, and on the possible influence of other sources of ionization. We have only tried the simplest possible assumption regarding the ionizing spectrum in modeling our warm absorber—a hard X-ray spectrum of the same shape as we measure with BBXRT. Given the various other possible choices of spectrum, we feel that a warm absorber cannot be excluded as a possible explanation for the absorption measured by BBXRT.

Although it is tempting to generalize these results to other similar objects, evidence from other observations suggests that BY Cam is not typical of magnetic CVs. One indication of this is the difference between the periods derived from Hα variability (Silber et al. 1992), and from polarimetry (Mason et al. 1989), which suggests that BY Cam is not a phase-locked system. If so, scenarios developed for intermediate polars may be considered in an effort to understand BY Cam. For example, it has been suggested that in intermediate polars a partial accretion disk may cause material to accrete over a very limited range of polar angle with respect to the magnetic axis (Hellier, Cropper, & Mason 1991), leading to a "curtain-like" geometry for the emission region above the white dwarf. This could account for the weakness of soft X-rays from BY Cam if the curtain tends to radiate preferentially in directions normal to its surface. Then we would observe a greater hard X-ray intensity than does the white dwarf.

In summary, we find the following: (1) Data from BBXRT observations of H0538+608 are consistent with those from past experiments in the continuum luminosity, temperature, and iron line strength and centroid energy. (2) The low-energy absorption shows an edge near 0.6 keV, which is consistent with neutral or partially ionized oxygen. Such an edge could arise from absorption by partially ionized material, or material with enhanced oxygen abundance relative to carbon and helium. (3) The spectrum below the edge is consistent with absorption by normal neutral material, with no evidence for a soft blackbody component exceeding 10% of the luminosity of the hard X-ray component for a blackbody temperature of 50 eV. (4) The iron K-line energy is consistent with partially ionized iron, with upper limits $\sim$0.1–0.3 from contributions by neutral or hydrogen-like ions. The absence of a neutral iron line is consistent with the lack of a soft blackbody component and argues against reprocessing of the hard X-rays on the surface of the white dwarf. Possible explanations for this include reprocessing in a hot optically thick layer on the white dwarf (although this is likely to produce a reprocessed continuum which is detectable at some level), and hard X-ray emission which is preferentially directed away from the white dwarf or which is approximately isotropic but occurs several stellar radii away from the white dwarf surface.

We thank the referee for several constructive comments and suggestions.

REFERENCES

Basko, M. 1977, ApJ, 223, 268
Bonnet-Bidaud, J. M., & Mouchet, M. 1987, A&A, 188, 89
Cropper, M. 1990, Sp. Sci. Rev., 54, 195
Forman, W., Jones, C., Cominsky, L., Julien, P., Murray, S., Tananbaum, H., & Giacconi, R. 1978, ApJS, 38, 357
Hatchett, S. P., & Weaver, R. 1977, ApJ, 215, 285
Hellier, C., Cropper, M., & Mason, K. O. 1991, MNRAS, 248, 233
Ishida, M., Silber, A., Bradt, H. V., Remillard, R. A., Makishima, K., & Ohashi, T. 1989, ApJ, 367, 270
Kallman, T. R. 1991, in Proc. Varenna Workshop on Iron Lines in Astrophysics, ed. A. Treves (Berlin: Springer)
Kallman, T. R., & Krolik, J. H. 1993, preprint
Kallman, T. R., & McCray, R. 1982, ApJ, 50, 263
Kallman, T. R., & White, N. E. 1989, ApJ, 341, 955
Krolik, J. H., & Kallman, T. R. 1984, ApJ, 286, 366
Makishima, M. 1986, in Accretion onto Compact Objects, ed. K. O. Mason, M. G. Watson, & N. E. White (Berlin: Springer), 249
Mason, P. A., & Chanmugam, G. 1992, in Vina Del Mar Workshop on Cataclysmic Variable Stars, ed. N. Vogt (ASP Conf. Series), 216
Mason, P. A., Liebert, J., & Schmidt, G. D. 1989, ApJ, 346, 941
Morrison, R., & McCammon, D. 1983, ApJ, 270, 119
Posdnyakov, L. A., Sobol, I. M., & Sunyaev, R. A. 1979, A&A, 75, 214
Remillard, R. A., Bradt, H. V., McClintock, J. E., Patterson, J., Roberts, W., Schwartz, D., & Tapia, S. 1986, ApJ, 302, L11
Savage, B., & Mathis, J. 1979, ARA&A, 17, 73
Serlemitsos, P. J., et al. 1991, in Proc. 21st Yamada Conf., First Results from BBXRT, in press
Shrader, C. R., McClintock, J. E., Remillard, R. A., Silber, A., & Lamb, D. Q. 1988, in A Decade of UV Astronomy with the *IUE* Satellite, ed. E. J. Rolfe, Vol. 1 (ESA SP-281, vol. 1)
Silber, A., Bradt, H. V., Ishida, M., Ohashi, T., & Remillard, R. A. 1992, ApJ, 389, 704
Swank, J. H., Fabian, A. C., & Ross, R. R. 1984, ApJ, 280, 734
Wood, K., et al. 1984, ApJS, 56, 507